The Canadian Mineralogist
Vol. 44, pp. 159-175 (2006)

COMPARATIVE CRYSTAL-STRUCTURE STUDY OF Ag-FREE LILLIANITE AND GALENOBISMUTITE FROM VULCANO, AEOLIAN ISLANDS, ITALY

DANIELA PINTO

Dipartimento Geomineralogico, University of Bari, Via E. Orabona 4, I-70125 Bari, Italy

TONČI BALIĆ-ŽUNIĆ

Departement of Mineralogy, Geological Institute, University of Copenhagen, Østervoldgade 10, DK-1350 Copenhagen K, Denmark

ANNA GARAVELLI

Dipartimento Geomineralogico, University of Bari, Via E. Orabona 4, I-70125 Bari, Italy

EMIL MAKOVICKY

Departement of Mineralogy, Geological Institute, University of Copenhagen, Østervoldgade 10, DK-1350 Copenhagen K, Denmark

FILIPPO VURRO[§]

Dipartimento Geomineralogico, University of Bari, Via E. Orabona 4, I-70125 Bari, Italy

ABSTRACT

The crystal structures of natural Ag-free lillianite of fumarolic origin from Vulcano, Aeolian Islands, Italy, $Pb_{2.88}Bi_{2.12}(S_{5.67}Se_{0.33})_{\Sigma 6.00}$, with *a* 13.567(1), *b* 20.655(2), *c* 4.1216(4) Å, *V* 1155.0(2) Å^3, space group *Bbmm*, *Z* = 4, and galenobismutite also from Vulcano, $Pb_{1.00}Bi_{2.03}(S_{3.87}Se_{0.11})_{\Sigma 3.98}$, with *a* 11.815(2), *b* 14.593(2), *c* 4.0814(6) Å, *V* 703.7(2) Å^3, space group *Pnam*, *Z* = 4, were refined from single-crystal X-ray data. The refinements converge to $R = 3.40\%$ [for 745 reflections with $F_o > 4\sigma(F_o)$], and $R = 2.96\%$ [for 607 reflections with $F_o > 4\sigma(F_o)$] for Ag-free lillianite and galenobismutite, respectively. In Ag-free lillianite, the trigonal prism *M*3 is occupied only by Pb, whereas both the octahedrally coordinated *M*1 and *M*2 sites are mixed (Pb,Bi) positions. The same octahedra incorporate both the surplus of Bi and vacancies (□) created by the substitution $3Pb^{2+} \rightarrow 2Bi^{3+} + \square$, which allows for the observed deviations from the ideal composition, $Pb_3Bi_2S_6$. Selenium is preferentially ordered at the six-fold and five-fold coordinated anionic sites, whereas the four-fold coordinated site S3 remains free of Se. The known structural arrangement of galenobismutite was confirmed in this work. The octahedrally coordinated $M1_{gb}$ site was found to be a full Bi position. Some evidence of Pb–Bi disorder has been observed at both the $M2_{gb}$ (Bi-dominated) and $M3_{gb}$ (Pb-dominated) positions. A heterogeneous distribution of Se in the anionic S sites was observed in galenobismutite. Atoms of Se are mainly concentrated at the site S1, and less so in the other anionic sites.

Keywords: Ag-free lillianite, galenobismutite, crystal structure, fumaroles, Vulcano, Italy.

SOMMAIRE

Nous avons affiné la structure de la lillianite naturelle dépourvue d'argent, d'origine fumerollienne, provenant de Vulcano, dans les îles Eoliennes, en Italie, $Pb_{2.88}Bi_{2.12}(S_{5.67}Se_{0.33})_{\Sigma 6.00}$, avec *a* 13.567(1), *b* 20.655(2), *c* 4.1216(4) Å, *V* 1155.0(2) Å^3, groupe d'espace *Bbmm*, *Z* = 4, et celle de la galénobismutite, du même endroit, $Pb_{1.00}Bi_{2.03}(S_{3.87}Se_{0.11})_{\Sigma 3.98}$, avec *a* 11.815(2), *b* 14.593(2), *c* 4.0814(6) Å, *V* 703.7(2) Å^3, groupe d'espace *Pnam*, *Z* = 4, au moyen de données en diffraction X prélevées sur monocristal. Les affinements ont convergé aux résidus $R = 3.40\%$ [745 réflexions avec $F_o > 4\sigma(F_o)$], et $R = 2.96\%$ [607 réflexions avec $F_o > 4\sigma(F_o)$] pour la lillianite sans Ag et la galénobismutite, respectivement. Pour la lillianite dépourvue de Ag, le prisme trigonal *M*3 ne contient que Pb, tandis que les deux sites octaédriques *M*1 et *M*2 ont une occupation mixte (Pb,Bi). Les mêmes octaèdres incorporent le surplus de Bi et les lacunes (□) créées par la substitution $3Pb^{2+} \rightarrow 2Bi^{3+} + \square$, ce qui rend compte des

§ *E-mail address*: f.vurro@geomin.uniba.it

écarts à la composition idéale, $Pb_3Bi_2S_6$. Le sélénium est ordonné de préférence aux sites anioniques à coordinence six et cinq, tandis que le site S3, à coordinence quatre, demeure dépourvu de Se. L'agencement des atomes de la galénobismutite, déjà connu, a été confirmé. Le site $M1_{gb}$, à coordinence octaédrique, ne contient que le Bi. Nous avons trouvé des signes de désordre Pb–Bi à la fois sur le site $M2_{gb}$ (à dominance de Bi) et $M3_{gb}$ (à dominance de Pb), et une distribution hétérogène de Se sur les sites anioniques S. Les atomes de Se sont surtout concentrés sur le site S1.

(Traduit par la Rédaction)

Mots-clés: lillianite dépourvue de Ag, galénobismutite, structure cristalline, fumerolles, Vulcano, Italie.

Introduction

A series of papers dealing with rare sulfosalts from Vulcano, Aeolian Islands, southern Italy, has been recently published (Borodaev *et al.* 1998, 2000, 2001, 2003, Vurro *et al.* 1999, Garavelli *et al.* 2005). The details of the geological settings and mineral assemblages in the high-temperature fumarole field of "La Fossa" crater of Vulcano can also be found in Garavelli *et al.* (1997). The assemblage mainly consists of Pb–Bi and Pb–Bi–As sulfides and sulfosalts, with subordinate Fe and Zn sulfides: pyrite–pyrrhotite and sphalerite–wurtzite. Among the sulfosalts, kirkiite, $Pb_{10}As_3Bi_3(S,Se)_{19}$ (Borodaev *et al.* 1998), cannizzarite–wittite with the compositional range $Pb_3(Bi_{4-x}Pb_x)_4(S_{9-y}Se_y)_{9-x/2}$, $0.04 \le x \le 0.28$, $0.5 \le y \le 3.5$ (Borodaev *et al.* 2000), Ag- and Cu-free lillianite, $Pb_3Bi_2(S,Se)_6$ (Borodaev *et al.* 2001), heyrovskýite, $Pb_6Bi_2(S,Se)_9$ (Borodaev *et al.* 2003), and the two new minerals mozgovaite, $PbBi_4(S,Se)_7$ (Vurro *et al.* 1999) and vurroite, $Pb_{20}Sn_2(Bi,As)_{22}S_{54}Cl_6$ (Garavelli *et al.* 2005) were described.

The rapid drop of temperature taking place at the fumaroles, similar to the quenching procedure in the synthesis of phases in laboratory experiments, allows the formation at Vulcano of generally very small crystals, which lack traces of decomposition, and commonly are homogeneous and well preserved. The invariable presence of selenium substituting for sulfur in all the analyzed phases, as well as the common incorporation of Cd in some of the minerals (Vurro *et al.* 1999, Borodaev *et al.* 2001, 2003), are due to the abundance of these elements in the fumarole fluids at the moment of the deposition. Analogously, the lack of monovalent cations (Ag or Cu), which are commonly admixed in natural Pb–Bi sulfosalts from other localities, is connected to the absence of Ag and Cu in fumarole fluids. The case of lillianite from Vulcano is particularly interesting, because it represents the first occurrence of this mineral with a close-to-ideal composition. All the other natural occurrences of lillianite contain variable amounts of Ag or Cu (or both) as a consequence of the easy heterovalent substitution 2 Pb → Ag(Cu) + Bi (Makovicky & Karup-Møller 1977a, b).

Here, we present results of the first structural investigations of Ag-free lillianite from Vulcano and of a re-investigation of the structure of galenobismutite from the same locality. The results of the refinements are discussed and compared with literature data. Furthermore, a comparative study of these structures is presented involving the geometry, occupancies and degree of distortion of their characteristic coordination-polyhedra.

Review of the Literature

Lillianite is the natural analogue of synthetic Phase III in the $PbS–Bi_2S_3$ system (Otto & Strunz 1968, Salanci & Moh 1969). The structure of this mineral was solved using both the synthetic Phase III of Otto & Strunz (1968) and natural Ag-bearing crystals (Takagi & Takéuchi 1972). Lillianite is the type mineral of the lillianite homologous series, which is an accretionary series of primarily Pb–Bi–Ag sulfosalts (Makovicky & Karup-Møller 1977a). The crystal structure of each lillianite homologue is characterized by the presence of alternating layers of the PbS archetype, cut parallel to the plane $(131)_{PbS}$, which also represent the reflection and contact plane of chemical twinning. Distinct homologues differ in the thickness of PbS-like layers, expressed by the number N of octahedra running diagonally across an individual layer of the archetype and parallel to $[011]_{PbS}$. Each lillianite homologue is denoted as $^{N1,N2}L$, where N_1 and N_2 are the values of N for two adjacent "pseudo-mirror" related layers. The value of N may be calculated directly from the chemical data (Nc) or, alternatively, it can be determined crystallographically. Makovicky & Karup-Møller (1997a, b) showed that the chemical composition of lillianite homologues can be expressed by the formula $Pb_{N-1-2x}Bi_{2+x}Ag_xS_{N+2}$, where $N = (N_1 + N_2)/2$ and x is the coefficient in the substitution 2 Pb ⇌ Ag(Cu) + Bi. Lillianite is the homologue $^{4,4}L$ of this series.

Structural investigations of galenobismutite from the Nordmark mines, Sweden, were performed by Wickman (1951) and by Iitaka & Nowacki (1962). Makovicky (1977) interpreted the crystal structure of galenobismutite as an incomplete lillianite-like structure $^{2,-}L$. According to this author, two-thirds of this structure represent in fact a distorted, contracted set of the lillianite linkage pattern. The structure of galenobismutite forms a pair of homologues with that of weibullite (Mumme 1980). Within the modular description (Makovicky 1981), these structures are interpreted as

members of a plesiotypic series composed of structures derived from cannizzarite (Makovicky 1997, Ferraris *et al.* 2004).

Experimental

Single crystals of Ag-free lillianite and of galenobismutite were chemically and structurally investigated. The two crystals examined were collected in the high-temperature fumarole field at Vulcano (lillianite is from fumarole FA, sampled June 1994, T = 520°C; galenobismutite is from fumarole FS, sampled June 1991, T ~550°C). The chemical compositions of crystals studied were obtained by electron-microprobe analysis using an ARL–SEMQ–95 instrument at the Centro Studi Geominerari e Metalurgici, CNR, Cagliari. Operating conditions were as follows: voltage 20 kV, beam current 20 nA; standards (emission lines): PbS (Pb*M*α, S*K*α), Bi_2S_3 (Bi*M*α), CdS (Cd*L*α), metallic Ag (Ag*L*α), CuS (Cu*K*α), $FeAsS_2$ (As*L*α), metallic selenium (Se*L*α), KCl (Cl*K*α), metallic Sn (Sn*L*α). Detection limits (in wt.%) were: Pb 0.10, S 0.02, Bi 0.10, Cd 0.14, Ag 0.05, Cu 0.04, As 0.08, Se 0.04, Cl 0.03. Both the Ag-free lillianite and galenobismutite crystals were found to be homogeneous within analytical error. Electron-microprobe results (wt.%) are reported in Table 1. The empirical formulae and Nc values, calculated for each composition, also are given.

The selected needle-like crystals of lillianite and galenobismutite were measured on a Bruker AXS four-circle diffractometer equipped with CCD 1000 area detector (6.25 cm × 6.25 cm active detection-area, 512 × 512 pixels) and a flat graphite monochromator using Mo*K*α radiation from a fine-focus sealed X-ray tube. Experimental and refinement data are summarized in Table 2. The SMART system of programs (Bruker AXS 1998) was used for unit-cell determinations, data collection and measurement of the crystal shapes. Data reduction, including intensity integration, background and Lorentz-polarization corrections, was carried out using the program SAINT Plus (Bruker AXS 1997a). A face-indexed absorption correction has been applied by means of the program XPREP from the SHELXTL package (Bruker AXS 1997b). The R_{int} factors after the face-indexed absorption correction were 6.16% and 8.97% for lillianite and galenobismutite, respectively, compared to the respective values of 9.5% and 12.0% before the absorption correction. The minimum and maximum X-ray transmission-factors were 0.10 and 0.51 for lillianite, and 0.20 and 0.55 for galenobismutite, respectively.

The structure refinements of Ag-free lillianite and galenobismutite from Vulcano were performed starting from atom coordinates for natural Ag-bearing lillianite (Takagi & Takéuchi 1972) and galenobismutite (Iitaka & Nowacki 1962), respectively, using the full-matrix least-squares program SHELXL–97 (Sheldrick 1997).

TABLE 1. CHEMICAL COMPOSITION OF Ag-FREE LILLIANITE AND GALENOBISMUTITE FROM VULCANO

	Pb	Bi	S	Se	Sum	Nc
			lillianite			
	48.17	35.27	14.55	2.03	100.02	3.75
	48.75	35.70	14.63	2.10	101.17	3.76
	48.14	35.64	14.69	2.09	100.56	3.72
	47.88	35.55	14.59	2.17	100.18	3.72
	47.27	35.57	14.68	2.02	99.54	3.68
	47.57	35.49	14.37	2.12	99.55	3.70
Mean	47.96	35.54	14.58	2.09	100.17	3.72
St. Dev.	0.52	0.15	0.12	0.06		
Empirical average formula[1]			$Pb_{2.88}Bi_{2.12}(S_{5.67}Sc_{0.33})_{\Sigma 6.00}$			
Theoretical formula based on Nc			$Pb_{2.85}Bi_{2.10}\square_{0.05}(S_{5.67}Se_{0.33})_{\Sigma 6.00}$			
Ideal formula			$Pb_3Bi_2S_6$			
			galenobismutite			
	27.12	55.89	16.09	1.03	100.13	1.98
	27.12	55.64	16.00	1.10	99.98[2]	2.00
	26.66	55.71	16.32	1.12	99.81	1.97
	27.55	54.96	16.59	1.23	100.33	2.01
Mean	27.11	55.55	16.25	1.12	100.06	1.99
St. Dev.	0.36	0.41	0.26	0.08		
Empirical average formula[3]			$Pb_{1.06}Bi_{2.03}(S_{3.87}Se_{0.11})_{\Sigma 3.98}$			
Ideal formula			$PbBi_2S_4$			

[1] The formula is calculated on the basis of 11 atoms; [2] 0.12 wt.% Ag is included in the sum; [3] The formula is calculated on the basis of seven atoms. The compositions are quoted in wt.%.

TABLE 2. INFORMATION ON DATA COLLECTION AND REFINEMENT FOR Ag-FREE LILLIANITE AND GALENOBISMUTITE FROM VULCANO

	Lillianite	Galenobismutite
	Data collection	
X-ray power, Mo*K*α	40 kV, 37 mA, 0.71073 Å	40 kV, 37 mA, 0.71073 Å
Temperature	297 K	298 K
Detector-to-sample distance	4 cm	4 cm
Crystal size (mm)	0.04 × 0.018 × 0.126	0.04 × 0.09 × 0.144
Active detection-area	6.25 × 6.25 cm^2	6.25 × 6.25 cm^2
Resolution	512 × 512 pixels	512 × 512 pixels
Number of frames	2240	2240
Rotation width per frame	0.3°	0.3°
Measurement time	20 s	20 s
Maximum covered 2θ	61.02° (d = 0.70 Å)	52.72° (d = 0.80 Å)
Unique reflections	1002	816
Reflections $I > 2\,\sigma_I$	745	607
R_{int} before absorption correction	9.5%	12.0%
R_{int} after absorption correction	6.16%	8.97%
R_σ [$F_o > 4\,\sigma$ (Fo)]	3.96%	6.22%
Range of h, k, l	$-19 \le h \le 19$	$-14 \le h \le 14$
	$-29 \le k \le 29$	$-18 \le k \le 18$
	$-5 \le l \le 5$	$-4 \le l \le 5$
	Refinement	
R [$F_o > 4\,\sigma$ (Fo)]	3.40%	2.96%
R (all data)	4.90%	4.54%
wR (on F_o^2)	8.04%	6.76%
WR (all data)	8.50%	7.39%
Goof	0.959	0.680
Number of least-squares parameters	42	47

A table of structure factors for each sample is available from the Depository of Unpublished Data, CISTI, National Research Council of Canada, Ottawa, Ontario K1A 0S2, Canada.

The refinement without any constraint of the occupancies at the metal sites allowed us to investigate the distribution of potential vacancies among the cation positions in the structure of the Ag-free lillianite (Table 3). A moderate negative correlation (–0.741) between the scale factor and the occupancy of the site *M*1 of lillianite was observed, as well as a moderate positive correlation (0.739) between the occupancies of *M*1 and *M*2 sites. No correlation larger than 0.6 was observed between occupancies and displacement parameters of *M*1 and *M*2.

As suggested by the results of the electron-microprobe study, small amounts of selenium are present in the measured crystals of lillianite [0.33 atoms per formula unit (*apfu*)] and galenobismutite (0.11 *apfu*). Therefore, the distribution of this element among the non-metal positions was investigated in both structures. The occupancies of the S sites were kept free during the refinements. The positions S1, S2, and in particular S4 in Ag-free lillianite yield slightly higher electron-density than the other sites; no indication of a heavier element resulted for the position S3. Consequently, the S1, S2 and S4 sites in Ag-free lillianite were refined as mixed (S,Se) positions. In the structure of galenobismutite, Se-for-S substitutions have been observed in all four anion positions (Table 3).

The crystal structure of Ag-free lillianite from Vulcano, orthorhombic *Bbmm*, has been refined to the agreement *R* value 3.40% for 745 reflections with $F_o > 4\sigma(F_o)$ [4.90% for all the 1002 unique reflections]. The refinement of galenobismutite, orthorhombic *Pnam*, converges to the *R* value of 2.96% for the 607 reflections with $F_o > 4\sigma(F_o)$ [4.54% for all the 816 unique reflections]. In both cases, the final refinement was performed with anisotropic displacement-factors for all the atoms.

Fractional coordinates, occupancies and anisotropic displacement parameters of the atoms are summarized in Table 3, whereas selected *M*–S distances are shown in Table 4. The unit-cell parameters are listed in Table 5 in comparison with data from the literature (Takagi & Takéuchi 1972, Iitaka & Nowacki 1962).

As the atom-displacement ellipsoid of *M*3 of lillianite is more anisotropic than that of other structural sites (elongate along [010]), and as the sum of valences for this site is lower than the expected value 2 (Table 6),

TABLE 3. ATOM COORDINATES AND ANISOTROPIC DISPLACEMENT PARAMETERS FOR Ag-FREE LILLIANITE AND GALENOBISMUTITE FROM VULCANO

Site	*x/a*	*y/b*	*z/c*	Occupancy	U_{11}	U_{22}	U_{33}	U_{12}	U_{eq}
				lillianite					
*M*1	0.09079(4)	0.13373(3)	½	0.980(4)	0.0222(3)	0.0228(3)	0.0173(3)	0.0009(2)	0.0207(2)
*M*2	0.36313(3)	0.04918(3)	½	0.982(4)	0.0180(3)	0.0259(3)	0.0149(3)	0.0004(2)	0.020(2)
*M*3	0.32578(7)	¼	0	1	0.0319(5)	0.0765(9)	0.0257(6)	0	0.0447(4)
S1	0.2368(2)	0.0953(2)	0	0.97(1)	0.022(2)	0.045(3)	0.015(2)	0.012(1)	0.027(1)
Se1	0.2368(2)	0.0953(2)	0	0.03(1)	0.022(2)	0.045(3)	0.015(2)	0.012(1)	0.027(1)
S2	0	0	½	0.96(2)	0.028(3)	0.021(3)	0.017(3)	0.003(2)	0.022(2)
Se2	0	0	½	0.04(2)	0.028(3)	0.021(3)	0.017(3)	0.003(2)	0.022(2)
S3	0.1836(3)	¼	½	1	0.020(2)	0.021(2)	0.022(3)	0	0.0209(9)
S4	0.4550(2)	0.1654(2)	½	0.93(1)	0.023(2)	0.022(2)	0.021(2)	0.003(1)	0.022(1)
Se4	0.4550(2)	0.1654(2)	½	0.07(1)	0.023(2)	0.022(2)	0.021(2)	0.003(1)	0.022(1)
				galenobismutite					
$M1_{gb}$	0.06791(6)	0.39037(4)	¼	1	0.0186(4)	0.0175(3)	0.0141(4)	0.0012(3)	0.0167(2)
$M2_{gb}$	0.10151(6)	0.90529(5)	¼	1	0.0234(4)	0.0266(4)	0.0113(4)	0.0008(3)	0.0204(2)
$M3_{gb}$	0.24696(7)	0.65307(5)	¼	1	0.0336(5)	0.0243(4)	0.0204(4)	0.0076(3)	0.0261(2)
S1	0.3352(4)	0.0152(3)	¼	0.95(1)	0.019(3)	0.021(2)	0.017(3)	0.003(2)	0.019(2)
Se1	0.3352(4)	0.0152(3)	¼	0.05(1)	0.019(3)	0.021(2)	0.017(3)	0.003(2)	0.019(2)
S2	0.2596(4)	0.2966(3)	¼	0.98(1)	0.017(3)	0.014(2)	0.013(3)	0.003(2)	0.014(2)
Se2	0.2596(4)	0.2966(3)	¼	0.02(1)	0.017(3)	0.014(2)	0.013(3)	0.003(2)	0.014(2)
S3	0.0560(4)	0.0931(3)	¼	0.97(1)	0.015(2)	0.019(2)	0.018(3)	-0.002(2)	0.017(2)
Se3	0.0560(4)	0.0931(3)	¼	0.03(1)	0.015(2)	0.019(2)	0.018(3)	-0.002(2)	0.017(2)
S4	0.0185(4)	0.7125(3)	¼	0.97(1)	0.017(3)	0.015(2)	0.014(2)	-0.003(2)	0.015(2)
Se4	0.0185(4)	0.7125(3)	¼	0.03(1)	0.017(3)	0.015(2)	0.014(2)	-0.003(2)	0.015(2)

Sites *M*1 and *M*2 in lillianite contain approximately equal amounts of Pb and Bi. *M*3 is a pure Pb site. $M1_{gb}$ is a pure Bi site, $M2_{gb}$ is Bi-dominated, and $M3_{gb}$, Pb-dominated, with substitutions of up to 25 at.%. See Table 6 and text for a detailed analysis of the substitutions.

a refinement with *M*3 moved out of the symmetry plane was tried (with an isotropic displacement parameter). The resulting *R* factor was found to be almost identical to that of an anisotropic refinement, and the influence on other parameters was negligible. The displacement of the two equivalent sites obtained with half occupancy from the mirror plane was 0.193 Å. However, the calculation of the valence sum for the split Pb site (*M*3) gave only a slight improvement over the site on the symmetry plane (1.85 instead of 1.81), which shows that the coordination change is not very significant. The above evidence suggests that the large anisotropy of the displacement parameters can be caused by a dynamic disorder of the *M*3 atom over the two close sites out of the symmetry plane, or be a consequence of large movements inside a large coordination polyhedron. No proof of a static disorder in the structure could be obtained from our data.

Owing to the negligible difference in the scattering powers of Pb and Bi, the distribution of these elements over the metal positions of the structures cannot be derived from diffraction by conventional measurements. Methods based on *M*–S bond lengths, bond-valence calculations and volumes of the coordination polyhedra are generally used to differentiate these atoms (Brown & Altermatt 1985, Armbruster & Hummel 1987, Hummel & Armbruster 1987, Berlepsch *et al.* 2001a, Makovicky *et al.* 2001). In this work, the distribution of Pb and Bi over the cation positions was determined from the bond-valence calculations using the formula: $s = \exp[(r_0 - r)/B]$, where r_0 is an element-pair-specific bond-valence parameter, r is the bond distance, and B is a constant equal to 0.37 (Brown & Altermatt 1985). The values of bond-valence parameters for the Bi–S and Pb–S bonds quoted by Brese & O'Keeffe (1991) are the same (2.55), which allows an easy estimation of occupancies from the calculated valence-sums for cation positions. In addition, the *M*–S distances for both lillianite and galenobismutite structures were compared with the element-specific hyperbolae for Pb and Bi (Berlepsch *et al.* 2001a). Occupancies of cation positions were interpreted on the basis of the volume of the circumscribed sphere, least-squared-fitted to the cation polyhedron (Vs) and the coordination polyhedron itself (Vp), as well as the values of volume eccentricity (ECCv), volume sphericity (SPHv) and volume distortion (υ) of each coordination polyhedron (Balić-Žunić & Makovicky 1996, Makovicky & Balić-Žunić 1998).

TABLE 4. INTERATOMIC DISTANCES IN Ag-FREE LILLIANITE AND GALENOBISMUTITE FROM VULCANO, AND COMPARISON WITH DATA FROM THE LITERATURE

		Lillianite				Galenobismutite	
		[1]	[2]			[3]	[4]
*M*1	– S3	2.712(3)	2.69	$M1_{gb}$	– S2	2.646(5)	2.63(1)
	– S4	2.841(2) × 2	2.80		– S1	2.965(3) × 2	2.99(2) × 2
	– S1	2.967(2) × 2	2.98		– S4	2.731(3) × 2	2.73(2) × 2
	– S2	3.024(1)	2.99		– S1	3.075(5)	3.12(1)
*M*2	– S4	2.706(3)	2.64	$M2_{gb}$	– S3	2.762(3) × 2	2.78(2) × 2
	– S1	2.845(2) × 2	2.82		– S3	2.793(4)	2.79(1)
	– S2	2.954(0) × 2	2.94		– S4	2.979(5)	3.00(1)
	– S1	3.278(4)	3.27		– S2	3.061(3) × 2	3.02(2) × 2
					– S1	3.193(5)	3.10(1)
*M*3	– S3	2.823(3) × 2	2.81	$M3_{gb}$	– S2	2.925(3) × 2	2.98(2) × 2
	– S4	3.220(2) × 4	3.25		– S1	3.026(3) × 2	3.01(2) × 2
	– S1	3.416(4) × 2	3.36		– S3	3.217(4) × 2	3.21(2) × 2
					– S4	2.834(5)	2.85(1)
					– S4	3.760(5)	3.76(1)

[1] Ag-free lillianite from Vulcano (this study); [2] Ag-rich lillianite (Takagi & Takéuchi 1972); [3] galenobismutite from Vulcano (this study); [4] galenobismutite from the type locality (Iitaka & Nowacki 1962). Bond lengths are quoted in Å.

Results: The Crystal Structure of Lillianite

The structure of Ag-free lillianite from Vulcano (Fig. 1) contains three independent metal positions (*M*1, *M*2 and *M*3). The *M*1 and *M*2 show a distorted octahedral coordination, and they form a chain of octahedra running diagonally across the PbS-like layers. The *M*3 site, which displays a standing bicapped trigonal–prismatic coordination, is situated on the mirror plane that connects the adjacent, mirror-related galena-type layers. The structural arrangement obtained is the same as that of the natural Ag-bearing lillianite described by Takagi & Takéuchi (1972), except for slight differences in the values of atom coordinates (Table 3) and interatomic distances (Table 4). The pair of bond lengths along $[001]_{PbS}$ of the galena submotif in the *M*2 site shows the main disagreement. These *M*–S distances are 2.706(3) Å and 3.278(4) Å in lillianite from Vulcano, compared to the values 2.64 Å and 3.27 Å given by Takagi & Takéuchi (1972). As a consequence, the sample of lillianite investigated here shows the horizontal diameter of the *M*2 octahedra equal to 5.984 Å, substantially longer than the value of 5.91 Å calculated from the data reported by Takagi & Takéuchi (1972). A slight increase of the other *M*2–S interatomic distances can also be observed. Analogously, some of the *M*1–S distances

TABLE 5. UNIT-CELL PARAMETERS OF Ag-FREE LILLIANITE AND GALENOBISMUTITE FROM VULCANO, AND COMPARISON WITH THE LITERATURE

	Lillianite		Galenobismutite	
Space group	*Bbmm*	*Bbmm*	*Pnam*	*Pnam*
a (Å)	13.567(1)	13.535(3)	11.815(2)	11.79
b (Å)	20.655(2)	20.451(5)	14.593(2)	14.59
c (Å)	4.1216(4)	4.104(1)	4.0814(6)	4.10
V (Å^3)	1155.0(2)	1136.0	703.7(2)	705.3
Z	4	4	4	4
Reference	1	2	1	3

References: 1 This study, 2 Takagi & Takéuchi (1972), 3 Itaka & Nowacki (1962).

TABLE 6. COMPARISON BETWEEN COORDINATION PARAMETERS (*) FOR CATION SITES IN Ag-FREE LILLIANITE AND GALENOBISMUTITE FROM VULCANO, AND COMPARISONS WITH THE LITERATURE

	CN	<d>	*d min*	*d max*	r_s	Vs	Vp	υ	ECCv	SPHv	Val.
Ag-free lillianite (this study)											
*M*1	6	2.9(1)	2.712(2)	3.024(1)	2.89(2)	101.362	32.08(5)	0.0057	0.1813	0.9792	2.53
*M*2	6	2.9(2)	2.706(3)	3.278(4)	2.94(4)	106.379	33.46(6)	0.0119	0.2741	0.9593	2.42
*M*3	8	3.2(2)	2.823(3)	3.413(4)	3.2(2)	133.455	55.4(1)	0.0428	0.1272	0.8027	1.81
Ag-rich lillianite (Takagi & Takéuchi 1972)											
*M*1	6	2.9(1)	2.687(3)	2.993(1)	2.87(3)	99.345	31.39(8)	0.0072	0.2048	0.9721	2.64
*M*2	6	2.9(2)	2.638(3)	3.273(4)	2.92(3)	103.993	32.65(9)	0.0138	0.3023	0.9702	2.59
*M*3	8	3.2(2)	2.809(4)	3.362(4)	3.2(2)	133.389	55.4(2)	0.0422	0.1786	0.8243	1.82
galenobismutite (this study)											
$M1_{gb}$	6	2.9(2)	2.646(5)	3.075(5)	2.86(1)	97.888	30.75(9)	0.0132	0.2693	0.9880	2.94
$M2_{gb}$	7	3.0(2)	2.762(3)	3.193(5)	2.95(5)	107.099	36.4(1)	0.1021	0.2453	0.9504	2.68
$M3_{gb}$	8	3.1(3)	2.834(3)	3.761(5)	3.1(2)	124.668	51.6(1)	0.0462	0.3311	0.8284	2.13
galenobismutite (Iitaka & Nowacki 1962)											
$M1_{gb}$	6	2.9(2)	2.634(5)	3.122(5)	2.87(1)	99.434	31.1(2)	0.0184	0.3003	0.9853	2.87
$M2_{gb}$	7	2.9(1)	2.780(4)	3.104(5)	2.93(5)	105.044	35.8(2)	0.0988	0.1975	0.9522	2.68
$M3_{gb}$	8	3.1(3)	2.851(5)	3.758(5)	3.1(2)	125.988	52.2(3)	0.0427	0.3264	0.8440	2.01
$PbIn_2S_4$ (Arriortua *et al.* 1983)											
In1	6	2.60(7)	2.514(9)	2.656(9)	2.60(3)	73.307	22.5(2)	0.0339	0.1267	0.9707	3.18
In2	6	2.7(1)	2.55(1)	2.90(1)	2.68(3)	80.247	24.8(2)	0.0307	0.1971	0.9658	2.61
	7	2.9(5)	2.55(1)	4.06(1)	2.9(5)	99.687	32.4(2)	0.1423	0.4286	0.5045	2.62
Pb	8	3.1(3)	2.67(1)	3.80(1)	3.1(2)	125.516	51.9(3)	0.0468	0.3357	0.8010	2.34
$CaFe_2O_4$ (Decker & Kasper 1957)											
Fe2	6	2.03(5)	1.980(2)	2.087(2)	2.030(6)	35.049	11.0(2)	0.0150	0.1164	0.9916	2.70
Fe1	6	2.05(3)	1.995(3)	2.071(2)	2.05(3)	36.159	11.2(2)	0.0238	0.0295	0.9580	2.55
Ca	8	2.45(9)	2.365(2)	2.577(3)	2.45(4)	61.317	25.6(2)	0.0383	0.1490	0.9482	2.21

<d> : average bond-distance, r_s: radius of the circumscribed sphere, Vs: volume of the circumscribed sphere, Vp: volume of the coordination polyhedron, υ: volume distortion, ECCv: volume-based eccentricity of the coordination, SPHv: volume-based sphericity of the coordination, Val.: valence.

* The polyhedron parameters for atom coordinations are defined in Balić-Žunić & Makovicky (1996) and in Makovicky & Balić-Žunić (1998). The bond-valence calculations were made using the parameters of Brese & O'Keeffe (1991). All calculations were done with the program IVTON (Balić-Žunić & Vicković 1996).

in the structure of lillianite from Vulcano increase as well. In the *M*3 site, the two capping S1 atoms are each 3.416(4) Å apart, whereas the *M*3–S4 and *M*3–S3 distances are 3.220(2) and 2.823(3) Å, respectively. The corresponding distances reported by Takagi & Takéuchi (1972) are: *M*3–S1= 3.36 Å, *M*3–S4 = 3.25 Å and *M*3–S3 = 2.81 Å.

The concentrations of Se refined for the mixed (S,Se) sites of lillianite from Vulcano are: 0.03(1) in S1, 0.04(2) in S2 and 0.07(1) in S4. No selenium was found in S3. This may be a reflection of the coordination characteristics of the sites. Site S3 is the only tetrahedral anion site, whereas S1 and S2 have octahedral, and S4, square pyramidal coordination. The resulting total Se is ~0.24 *apfu* (for a total of 6 atoms), which is less than the amount of this element obtained by electron-microprobe investigations [0.33(1) *apfu*]. The disagreement could be ascribed to the difficulty in refining such a low concentration with a high degree of accuracy. On the other hand, the relatively low residual *R* value (3.40%) supports the results of the refinement.

Owing to the larger size of Se^{2-} compared to S^{2-}, *M*–S distances will generally increase with the percentage of Se-for-S substitution. This is also suggested by the comparison between bond lengths in the sulfides PbS and Bi_2S_3 (Kupčik & Veselá-Nováková 1970) and the distances in the corresponding selenides PbSe and Bi_2Se_3 (Atabaeva *et al.* 1973). The values of the shortest *M*–S distances in the sulfides (2.960 and 2.669 Å, respectively) are significantly shorter than the corresponding

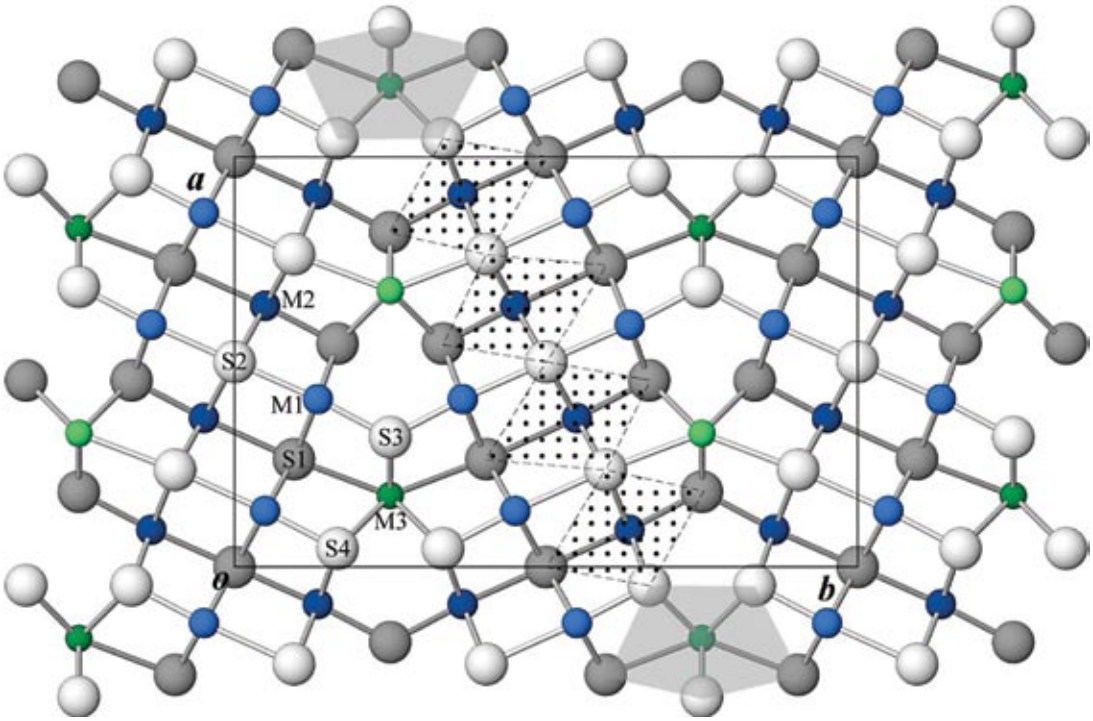

FIG. 1. The crystal structure of Ag-free lillianite from Vulcano. Projection on (001). Blue circles: mixed (Pb,Bi) positions, green circles: Pb positions, grey circles: S positions. Lightly and darkly shaded circles indicate atoms at z = ½ and z = 0, respectively, along the ~4 Å axis. Stippled: chain of N octahedra running diagonally across an individual PbS-like layer, grey shades: bicapped trigonal prisms of *M*3.

ones in the selenides (3.06 and 2.819 Å, respectively). This might explain the previously described stretching of the *M*–S distances in *M*1 and *M*2.

Another expected consequence of the incorporation of selenium in lillianite is an increase of the unit-cell size. This is confirmed by the analysis of unit-cell parameters obtained by Liu & Chang (1994) for several samples of synthetic Ag-free lillianite with variable selenium contents, which allows us to establish a positive linear correlation between the cell parameters and selenium content (Fig. 2). Unfortunately, no reliable X-ray data for additional natural occurrences of selenian lillianite are available. Analysis of the graphs reported in Figure 2 shows that the cell expands proportionately in all directions with the increase of Se. The unit-cell parameters of the natural Ag-free selenian lillianite investigated in this work conform very well to the relations outlined (Fig. 2). The same is observed for the synthetic Phase III, investigated by Otto & Strunz (1968) and, partially, for the Ag-bearing lillianite studied by Takagi & Takéuchi (1972). The latter shows a *b* parameter significantly shorter than expected from the correlation line in Figure 2b. This is explained by the incorporation of Ag. Makovicky & Karup-Møller (1977b) first, and Borodaev *et al*. (2001) later, suggested that the *b* parameter of lillianite decreases linearly with the percentage of the (Ag + Bi)-for-(2Pb) substitution, as in the PbS–$AgBi_2S_2$ solid solution.

The selected sample of lillianite from Vulcano differs from the ideal composition, $Pb_3Bi_2S_6$, by showing a slight surplus of bismuth. The value of chemical N calculated for the mean composition (Nc = 3.72) is less than the crystallographically defined theoretical value (N = 4). Makovicky (1981) noted that differences between non-integral values of N, generally smaller than the theoretical one, may be due either to vacancies in the metal positions, created by the substitution $3Pb^{2+} \rightarrow 2Bi^{3+} + \square$ (□: vacancy), or to errors in the frequency of "chemical twinning". In Table 1, the empirical chemical formula of Ag-free lillianite with vacancies (□) also is reported. The amount of vacancies has been calculated from the general formula of the lillianite homologous series, $Pb_{N-1-2x}Bi_{2+x}Ag_xS_{N+2}$, considering x = 0 and N = 3.72. The number of vacancies in Ag-free lillianite from Vulcano [□ = 0.05 per formula unit (*pfu*)] is very small. In any case, the good quality of the data allowed the refinement of vacancies. No preference in distribution of vacancies was noted

in any of the (Pb,Bi) mixed sites (*M*1 and *M*2), both of which were found to contain ~0.02 □ *pfu*. A total of vacancies equal to 0.08 *pfu* was calculated, which is a value higher than that suggested by the chemical composition. The discrepancy can be ascribed to the small number of vacancies at each site, which is close to the limit of resolution of the refinement.

Bond-valence calculations (Table 6) clearly suggest a mixed (Pb,Bi) occupancy for both *M*1 and *M*2 octahedron sites of lillianite, whereas the *M*3 site appears to be occupied only by Pb. This is in agreement with Takagi & Takéuchi (1972), and is confirmed by the plot in Figure 3. The *M*1 and *M*2 pairs of bond lengths, which represent the bond lengths in the $(001)_{PbS}$ plane, plot between the curves of Bi and Pb. The *M*1 pair of bond lengths along $[001]_{PbS}$ plot closer to the hyperbola of bismuth than does the *M*2 pair (Fig. 3). This may be ascribed to a lower content of the element with a more active lone-electron pair (Bi) in *M*2 than in *M*1. Consequently, the *M*2 site in the Ag-free lillianite seems to be richer in Pb than *M*1. The higher Vs and Vp volumes observed for the *M*2 site, if compared to those of *M*1 site (Table 6), support this conclusion. On the other hand, the difference between the longest and the shortest bond of *M*2, which is larger than the same difference calculated for *M*1, as well as the greater eccentricity and the lower sphericity of *M*2 compared to those of the *M*1 site, strongly suggest a preference for Bi in *M*2. This result is in agreement with that of Ohsumi *et al*. (1984), who studied the degree of Pb–Bi order in a sample of Ag-bearing lillianite by means of a synchrotron radiation with a wavelength equal to 0.96 Å. From the differ-

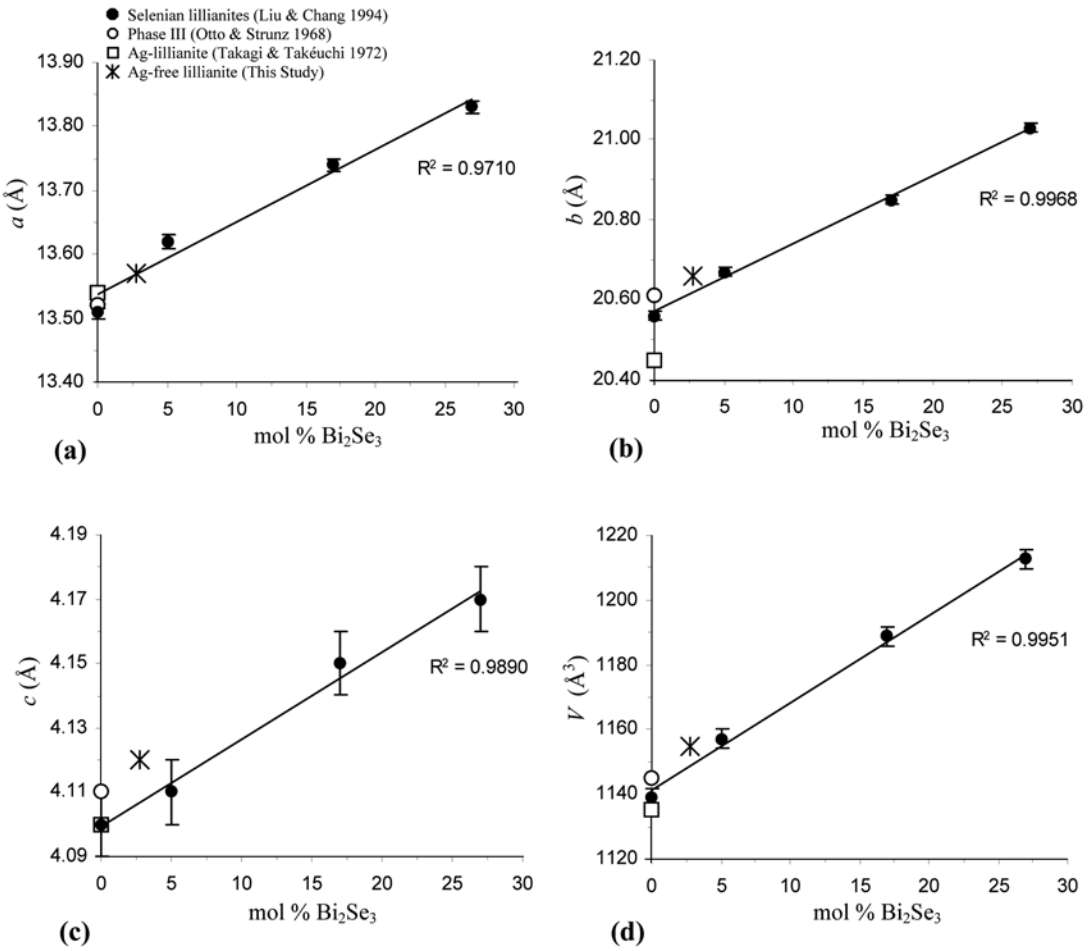

FIG. 2. Linear correlations between cell parameters (Å) and Se content (expressed in mol.% Bi_2Se_3) in synthetic compositions of selenian lillianite (Liu & Chang 1994). The cell parameters of selenian lillianite from Vulcano are indicated by an asterisk.

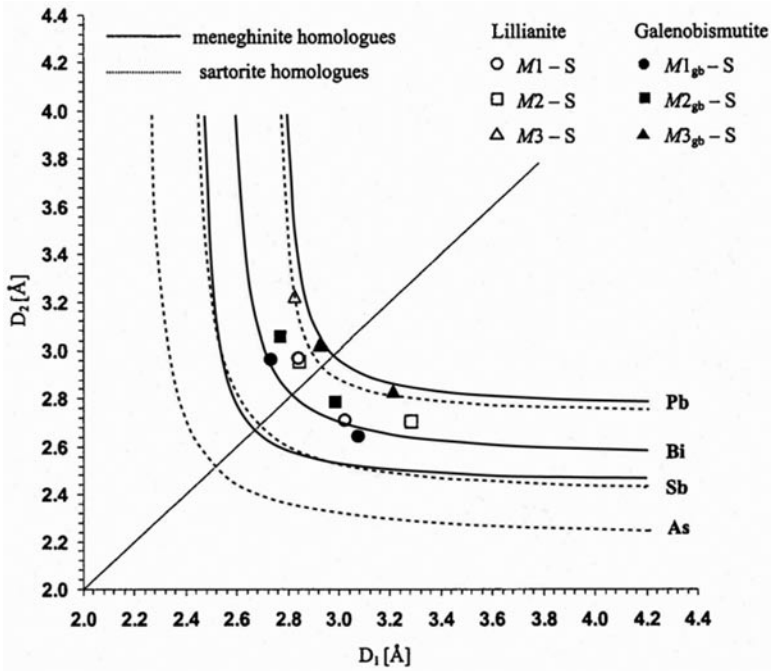

FIG. 3. Element-specific bond-length hyperbolae for pairs of opposing bonds (Berlepsch *et al*. 2001a) with individual bond-length data of Ag-free lillianite and galenobismutite added. Each pair of bond lengths consists of a short (x_n) and an opposing long (y_n) *M*–S bond distance (where $x_n < y_n$ and n = 1, 2, 3). Points P_1 (x_1y_1) ≡ P_2 (x_2y_2) above the median line indicate bond lengths in the plane $(001)_{PbS}$ of the galena submotif, and $P_3(y_3x_3)$ below the median line indicate bond lengths along $[001]_{PbS}$ of the galena submotif for each coordination polyhedron.

ence in the anomalous dispersion effects of Bi and Pb at this wavelength, they derived a preference for Bi for the *M*2 position. However, these authors did not report any quantitative refined data about the distribution of Pb and Bi in the mixed sites of lillianite obtained from their experiment. The assignment of 0.54 Pb and 0.46 Bi at *M*1 and 0.54 Bi and 0.46 Pb at *M*2 was obtained by Takéuchi (1997) from bond-valence calculations. The valence sums recalculated on the basis of the structural data reported by Takagi & Takéuchi (1972) but using the parameters quoted by Brese & O'Keeffe (1991) give the following occupancies: 0.36 Pb and 0.64 Bi at *M*1, and 0.59 Bi and 0.41 Pb at *M*2. This calculation ignores a small amount of Ag, which must have been present in this structure, on the basis of its unit-cell parameters, but which was not considered by Takagi & Takéuchi (1972).

In spite of the greater occupancy of Pb suggested for the *M*1 position, the polyhedron volume calculated for this position is smaller than that of the *M*2 site in both the structures of the Ag-free and Ag-bearing lillianite (Table 6). This finding is explained by the accommodation of the small lone-electron-pair micelles of Bi in the inner space between the two columns of *M*2 coordination pyramids. It is confirmed by the asymmetry of the complete *M*2 polyhedra, which shows that the longest *M*–S distance is the one crossing the micelles, and the shortest distance is opposite to them. The space of the structure where the polyhedra *M*2 occur thus is expanded and, as a consequence, the polyhedra *M*1 are compressed. In Ag-bearing lillianite, the incorporation of Ag at *M*1 (Makovicky 1977) causes a further reduction in the volume of this polyhedron.

The recently solved structure of the lillianite dimorph xilingolite, $Pb_3Bi_2S_6$ (Berlepsch *et al*. 2001b), offers important data about a possible ordering of Pb and Bi in the structure of lillianite. The structure of xilingolite is very close to that of lillianite, representing a monoclinic variant with an almost complete order of Pb and Bi among the structural positions. The main features of the two structures are the same, with the same types of coordination, and with small geometrical differences, according to an almost full ordering of cations. In xilingolite, the sites that correspond to *M*1

and *M*2 in lillianite are predominantly occupied by Bi or Pb in the alternating structural slabs. On average, there are thus similar occupancies in both types of structural sites throughout the structure, in accordance with the result for lillianite. Site *M*3 is a pure Pb site, again in accordance with lillianite, but in xilingolite, it shows a lower symmetry with a significant displacement of Pb from the center of the prism, which has the consequence that the coordination number is reduced to 7, and the prism is monocapped. In xilingolite, the bond-valence calculations for this site give an expected valence. This supports a conclusion that the observed deficit in the summary valence for the *M*3 site in lillianite, plus a high anisotropy of the atomic displacement factor with longest displacement axis oriented perpendicular to (010), are a consequence of a static or dynamic disorder of Pb at this site between two close positions on both sides of the (010) mirror plane, which produces a coordination situation similar to that in xilingolite. However, as already said in the experimental part, no proof of a static disorder in the structure that could be related to "xilingolite-like" domains could be obtained from our data.

Formally, the observed structure of lillianite can be regarded as a product of the unit-cell twinning of the xilingolite structure, or of a completely disordered stacking of the xilingolite structural slabs (as regards the occupancies and geometry of coordinations of cations). The observed Pb–Bi occupancies in the two structures are in accordance with these models. Both models support *M*3 as a pure Pb site, whereas for *M*1 and *M*2, a similar occupation of Pb and Bi is suggested. The observation that the vacancies are distributed equally between *M*1 and *M*2 sites is also consistent with this conclusion.

Results: The Crystal Structure of Galenobismutite

The structural study of galenobismutite from Vulcano is a refinement of the structure originally solved by Wickman (1951) and Iitaka & Nowacki (1962). This study confirms the general structural arrangement of galenobismutite; there are three independent cation-positions (Fig. 4). One metal position is characterized by a slightly distorted octahedral coordination ($M1_{gb}$), forming fragments of galena-like structure two octahedra wide. The second site is a lying-flat monocapped trigonal prism ($M2_{gb}$); the third metal position shows a standing trigonal prismatic coordination ($M3_{gb}$), with the cation surrounded by seven sulfur atoms with distances ranging from 2.834(5) to 3.217(4) Å, and one additional sulfur atom S4 at 3.760(5) Å. The rows of $M3_{gb}$ polyhedra, which run parallel to [001], are interconnected by long $M3_{gb}$–S4 contacts into undulating layers parallel to (010). The two $M2_{gb}$ polyhedra are paired around a center of symmetry, so that they share their S3 atoms. The $M2_{gb}$–S3 distances represent the three shortest bonds of the coordination polyhedron $M2_{gb}$. Consequently, the volume defined by the $M2_{gb}$ and S3 atoms is relatively small. This is a typical feature of the structure of galenobismutite. In fact, it is more common among sulfosalts that a similar connection between adjacent polyhedra is obtained by a combination of short and long bonds (*i.e.*, the central parts of the Bi_4S_6 ribbons in bismuthinite). A configuration similar to that of galenobismutite is present in the synthetic compound BiSCl (Voutsas & Rentzeperis 1980; Fig. 5), where all the short bonds are Bi–S bonds.

The concentrations of Se refined for the mixed (S,Se) sites of galenobismutite from Vulcano are: 0.05(1) in S1, 0.02(1) in S2, 0.03(1) in S3, and 0.03(1) in S4. The resulting total Se is ~0.13 *apfu*, which is in excellent agreement with the amount of Se obtained by electron-microprobe investigations [0.11(1) *apfu*]. This quantity is substantially lower than the concentration of selenium found in lillianite. The influence of selenium on *M*–S bond-lengths and unit-cell size has been previously discussed. In spite of the generally expected increase in cell parameters and *M*–S distances, no clear evidence of increase has been noted in this case. The unit-cell parameters of selenium-bearing galenobismutite from Vulcano are comparable with those from the literature (Table 5). A similar behavior is generally observed for the bond lengths (Table 4). Minor discrepancies can be explained by the different accuracy of the structural data. The lack of significant increase in the cell size and bond lengths can be ascribed to the small quantity of selenium in the sample of galenobismutite investigated, so that its effects on the structure are within the error limits.

The bonding-hyperbola diagram (Fig. 3) contains also data for galenobismutite from Vulcano. The pairs of selected opposing bonds for $M1_{gb}$ and $M3_{gb}$ sites suggest at the outset that the $M1_{gb}$ site is totally occupied by Bi, whereas $M3_{gb}$ is a fully occupied Pb site. The pairs of bonds for $M2_{gb}$ plot between the Bi and Pb curves, suggesting that $M2_{gb}$ is a mixed (Pb,Bi) position. The results of bond-valence calculations and the analysis of the coordination parameters for these cation sites lead to the same conclusion.

The polyhedron $M1_{gb}$ is characterized by a polyhedron volume (Vp) indicative of a full occupancy by Bi. The same evidence is also suggested by the relatively high value of eccentricity (ECCv), as well as by the value of the shortest *M*–S distance. The volume of the polyhedron $M3_{gb}$ is smaller than the value expected for a polyhedron with the same CN and with Pb as cation (*e.g.*, Vp of *M*3 in lillianite); the value of the eccentricity is relatively high (Table 6), suggesting the substitution of Bi for Pb at the $M3_{gb}$ site of galenobismutite. On the contrary, the value of the shortest bond in the polyhedron $M3_{gb}$ (Table 6) is more consistent with a full Pb occupancy.

Analysis of bond lengths of galenobismutite indicates that the three shortest *M*–S distances of the poly-

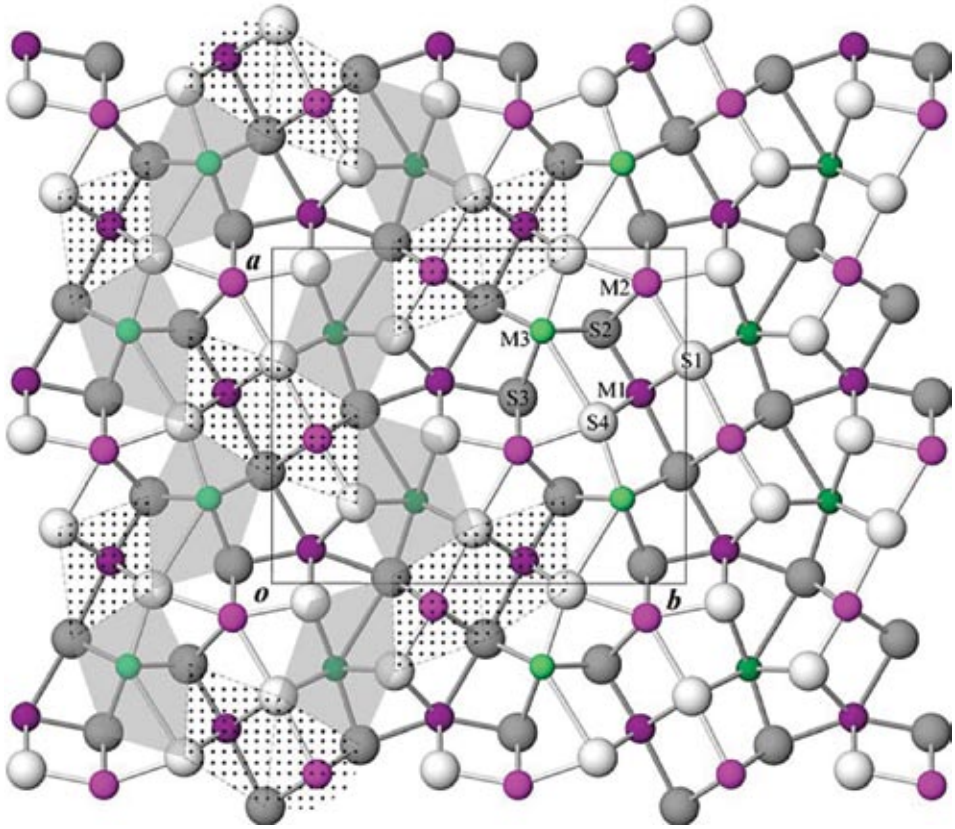

FIG. 4. The crystal structure of galenobismutite from Vulcano. Projection on (001). Pink circles: Bi-dominated sites, green circles: Pb-dominated sites, grey circles: S sites. Lightly and darkly shaded circles indicate atoms at $z = ¼$ and $z = ¾$, respectively, along the ~4 Å axis. The portions of lillianite-like octahedra are stippled, and the bicapped trigonal prisms of $M3_{gb}$ are shaded grey.

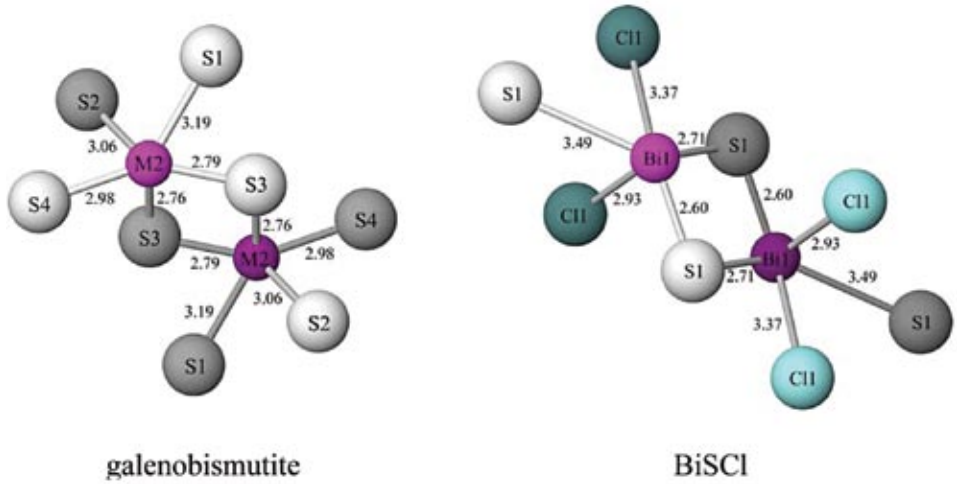

FIG. 5. Comparison between the coordination of the $M2_{gb}$ site in galenobismutite from Vulcano and the coordination of Bi in BiSCl (Voutsas & Rentzeperis 1980).

hedron $M2_{gb}$ ($M2_{gb}$–S3 distances, Table 4) are longer than those expected for a Bi atom [*i.e.*, Bi–S bonds in the compound BiSCl: 2.605(2) Å and 2.711(1) × 2 Å (Voutsas & Rentzeperis 1980)]. The evidence of relatively long $M2_{gb}$ – S3 distances in galenobismutite may be due to the partial Pb-for-Bi substitution at the $M2_{gb}$ site. This is confirmed by the results of bond-valence calculations (Table 6) and the diagram of the bond-lengths hyperbolae (Fig. 3), which suggest a mixed (Pb,Bi) occupancy for $M2_{gb}$. Considering the composition of the mineral (Table 1), and assuming that the $M1_{gb}$ site of galenobismutite is fully occupied by Bi, we must conclude that no mixed occupancy is possible for $M2_{gb}$ alone, unless accompanied by mixed occupancy at $M3_{gb}$.

We may conclude that $M1_{gb}$ is a pure Bi site, whereas $M2_{gb}$ and $M3_{gb}$ are dominated by Bi and Pb, respectively, with up to about 25% substitution by the other element.

Comparison Between the Structures of Lillianite and Galenobismutite

According to Makovicky (1977), a relationship exists between the crystal structures of lillianite homologues and galenobismutite. As in lillianite, the structure of galenobismutite is composed of blocks of PbS-like archetype surrounding a central "row" of bicapped trigonal prisms. However, in galenobismutite, a glide plane replaces the mirror plane characteristic of the lillianite series (Figs. 6a, d). Consequently, the two octahedra $M1_{gb}$ forming the PbS-like rod in galenobismutite do not have a symmetrical counterpart on the other side of the row of trigonal prisms $M3_{gb}$. In the space of the structure that should be occupied by the opposite galena-like layer (in a ^{2,2}L homologue, *i.e.*, Ti_2CaO_4, Fig. 6d), a pair of coordination polyhedra $M2_{gb}$ occurs.

Two thirds of the structure of galenobismutite can be interpreted as a distorted $^{2,-}$L structure (Makovicky 1977): the octahedron $M1_{gb}$ is analogous to both the *M*1 and *M*2 sites in the structure of lillianite ^{4,4}L, whereas the bicapped trigonal prism $M3_{gb}$ is "similar" to the *M*3 site in lillianite. The other metal position, $M2_{gb}$ (lying monocapped trigonal-prism), does not correspond to the lillianite motif.

The correlation between *M*–S distances in the structure of lillianite and the corresponding distances in galenobismutite from Vulcano is illustrated in Figures 7a and b. The three shortest *M*–S distances in the octahedron $M1_{gb}$ of galenobismutite (Fig. 7a) are significantly shorter than the corresponding distances in *M*1 and *M*2 octahedra of lillianite. The $M3_{gb}$ trigonal prism in galenobismutite is asymmetric, and appears more strained than the corresponding symmetric polyhedron in the structure of lillianite (Fig. 7b). This can be explained by the observation that in the structure of galenobismutite, the polyhedra $M2_{gb}$ form a distorted part of the structure, and the polyhedra $M1_{gb}$, a much less distorted part. This leads to a distortion and rotation of the polyhedra $M3_{gb}$ in the structure of galenobismutite, forming a zig-zag "row" along [100]. Consequently, the $M3_{gb}$ polyhedron in galenobismutite is closer to a monocapped trigonal prism than the corresponding polyhedron in lillianite (*M*3), which is a bicapped trigonal prism.

If the average of the two bond lengths of the capping S atoms in the $M3_{gb}$ sites of galenobismutite is plotted against the distance of the caps in the *M*3 site of lillianite (Fig. 7b), the resulting point is linearly and positively correlated with the other points in the diagram. The regression line obtained is not parallel to one described by a perfect 1:1 relationship; the slope and the rightward shift of the line from one going through the origin reflect the presence of Bi in the $M3_{gb}$ site. The *M*3 site in lillianite is supposed to be a pure Pb position.

A comparison of the coordination polyhedra in the structures of lillianite and galenobismutite shows that all coordination polyhedra in the structure of galenobismutite are more distorted and asymmetrical than the corresponding ones in the structure of lillianite. This is suggested by the comparison of the parameters υ (volume distortion) and ECCυ (volume eccentricity), both of which are greater in galenobismutite than in lillianite (Table 6).

According to Makovicky (1977), the deformation of the structure of galenobismutite ($^{2,-}$L) is produced by the necessity to accommodate the volume occupied by the lone-electron pairs of the two bismuth atoms within the potentially galena-like layer.

Relationship of Galenobismutite with Other Sulfosalt Structures

The crystal structure of galenobismutite shows strong similarity with the structure of $CaFe_2O_4$ (Decker & Kasper 1957, Mumme 1980, Makovicky 1977, 1981) and $PbIn_2S_4$ (Arriortua *et al.* 1983). The structural arrangement of these compounds is closely related to the linkage pattern of the lillianite homologue ^{2,2}L (Fig. 6).

The position $M3_{gb}$ in the structure of galenobismutite (Fig. 6a) corresponds to the largest cation, *i.e.*, Ca in $CaFe_2O_4$ (Fig. 6c), and Pb in $PbIn_2S_4$ (Fig. 6b). The coordination parameters (degree of distortion, eccentricity, sphericity and polyhedron volume) of the $M3_{gb}$ site of galenobismutite are very similar to those calculated for the Pb position in the compound $PbIn_2S_4$ (Table 6). On the other hand, it must be stressed that the polyhedron of Pb in $PbIn_2S_4$ is characterized by an unusually short *M*–S distance (Pb–S1= 2.67 Å), and that the sum of valences calculated for this position is substantially greater than the value expected. This might suggest a mixed (Pb,In) occupancy.

The coordination polyhedron of Ca in $CaFe_2O_4$ is more symmetrical than the corresponding one in galenobismutite and in $PbIn_2S_4$. It is characterized by a lower volume-distortion, lower eccentricity and greater sphericity than the corresponding values in the other structures (Table 6).

The octahedron $M1_{gb}$ of galenobismutite is more irregular than the octahedra In1 and Fe2 in the synthetic compounds $PbIn_2S_4$ and $CaFe_2O_4$, respectively. Polyhedron $M1_{gb}$ has the greatest value of eccentricity of the three polyhedra, and its volume distortion is quite similar to that of Fe2 in $CaFe_2O_4$. The polyhedron In1 is characterized by a volume distortion slightly greater than those of the polyhedra $M1_{gb}$ and Fe2 (Table 6).

The seven-fold coordinated position $M2_{gb}$ is replaced by a six-fold distorted octahedral coordination in the structures of $PbIn_2S_4$ and $CaFe_2O_4$ (In2 and Fe1, respectively). The comparison between these positions reveals a progressive increase of distortion, starting from the polyhedron Fe1 in $CaFe_2O_4$ and ending to $M2_{gb}$ in galenobismutite. In the latter, the octahedron is completely distorted, and a different type of coordina-

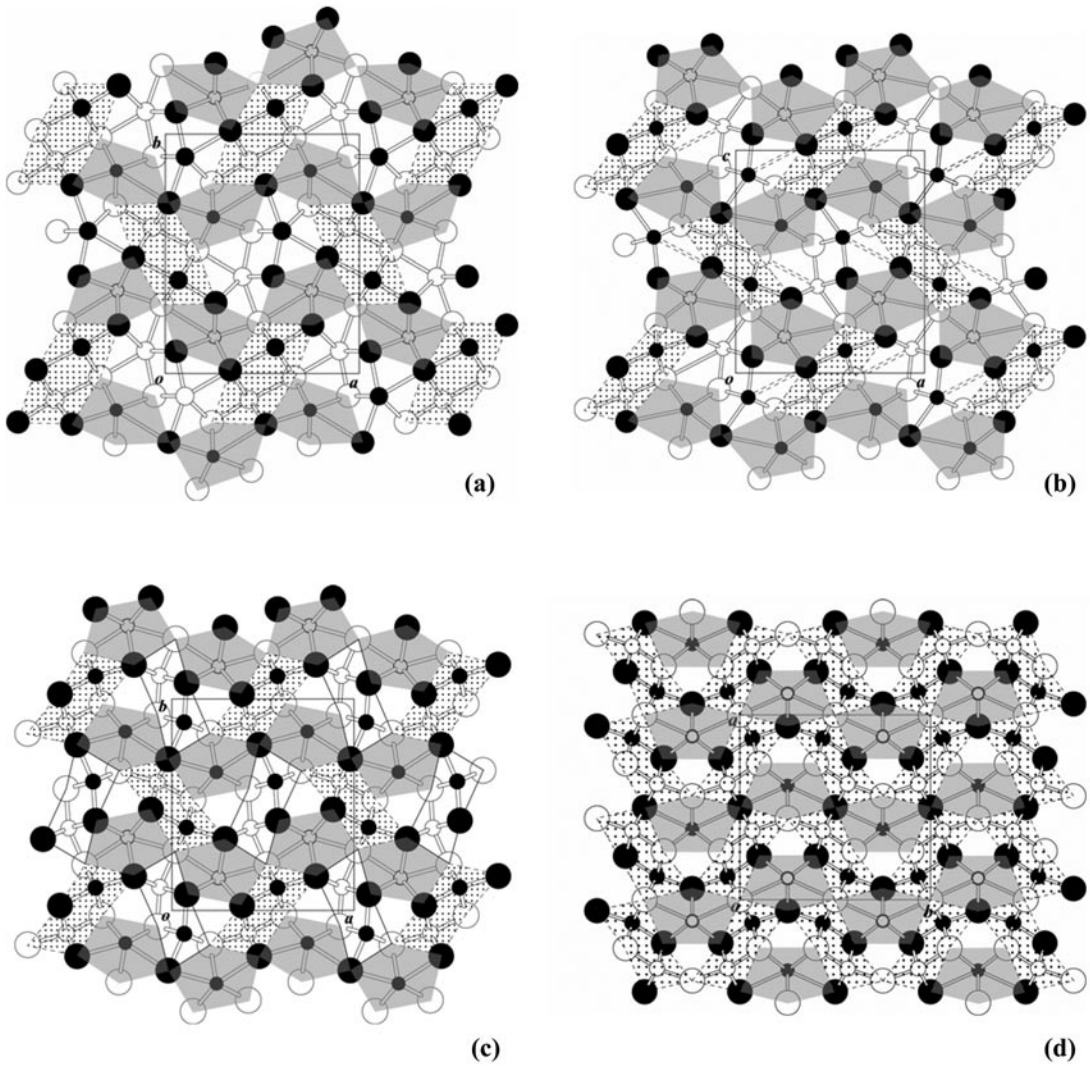

FIG. 6. The crystal structures of: a) galenobismutite $Pb_{1.00}Bi_{2.03}(S_{3.87}Se_{0.11})_{\Sigma 3.98}$ (this study), b) $PbIn_2S_4$ (Arriortua *et al*. 1983), c) calcium ferrite $CaFe_2O_4$ (Decker & Kasper 1957), d) Ti_2CaO_4 (Bertaut & Blum 1956). The structures in b), c), and d) show structural arrangements that correspond in part to the linkage pattern of the lillianite homologue N = 2. The portions of lillianite-like octahedra are stippled, the bicapped trigonal prisms are shaded grey.

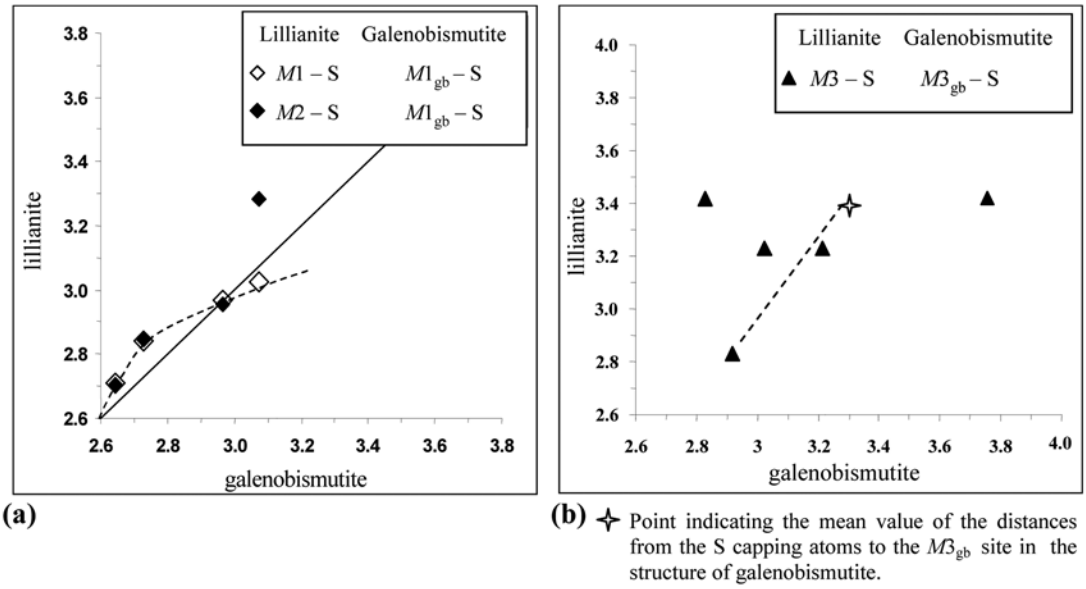

FIG. 7. a) Interatomic distances at the octahedron sites (*M*1 and *M*2) of Ag-free lillianite *versus* the corresponding distances in the octahedron $M1_{gb}$ of galenobismutite. b) Interatomic distances at the *M*3 site of the Ag-free lillianite *versus* the corresponding distances at the $M3_{gb}$ site of galenobismutite.

tion occurs (namely a monocapped trigonal prism, or "split octahedron").

Additional similarities exist among the structure of galenobismutite and those of some rare-earth sulfides and sulfosalts. The configuration of the two columns of lying-flat monocapped trigonal prisms $M2_{gb}$ and their two neighboring standing bicapped trigonal prisms, $M3_{gb}$, forms a lozenge-like rod (Fig. 8a), which is an element that occurs, variously stacked, in Gd_2S_3 (Fig. 8b), $CeTmS_3$ and $La_{10}Er_9S_{27}$, as well as in $Pb_4In_3Bi_7S_{18}$ (Makovicky 1992).

CONCLUDING REMARKS

The X-ray single-crystal study performed on a selected sample of Ag-free lillianite from Vulcano $[Pb_{2.88}Bi_{2.12}(S_{5.67}Se_{0.33})_{\Sigma 6.00}$, Nc = 3.72], allowed us to investigate the Pb–Bi order in the structure of lillianite in the absence of Ag. The study of the distribution of Pb and Bi over the metal positions of the structure of Ag-free lillianite has been performed using a combination of several approaches (bond-valence calculations, bond-length hyperbolae, analysis of coordination characteristics such as polyhedron volume, polyhedron distortion, eccentricity and sphericity of the coordination polyhedra). The trigonal prism *M*3 is occupied only by Pb, whereas both octahedrally coordinated *M*1 and *M*2 sites are mixed (Pb,Bi) positions. The admixture of Se is shown to be preferentially ordered at the six-fold and five-fold coordinated anionic sites, whereas the four-fold coordinated site S3 remains free of Se. The mixed character of the *M*1 and *M*2 sites, and the characteristics of the *M*3 coordination, can be explained, in comparison with the structure of xilingolite, as characteristics of the lillianite dimorph, in which the *M*3 site represents a mirror-symmetric compromise between the two "twinned" asymmetric Pb coordinations in xilingolite, and both *M*1 and *M*2 have characteristics of the overlapped dominantly Pb or dominantly Bi sites from the structure of xilingolite. Indications were found for a preference of Pb for the *M*1 site and Bi for the *M*2 site.

The present re-investigation of the structure of galenobismutite, performed by using a modern diffractometer with an area detector, allowed us to obtain atom coordinates and bond lengths of a high degree of accuracy. The general structural arrangement reported by Iitaka & Nowacki (1962) for galenobismutite was confirmed. As in the case of lillianite, metal occupancies were investigated. The $M1_{gb}$ site of galenobismutite is clearly a full Bi position. Although some evidence of Pb–Bi disorder has been observed in both the $M2_{gb}$ (Bi-dominated) and $M3_{gb}$ (Pb-dominated) positions, the data presented in this paper do not allow us to prove it definitively.

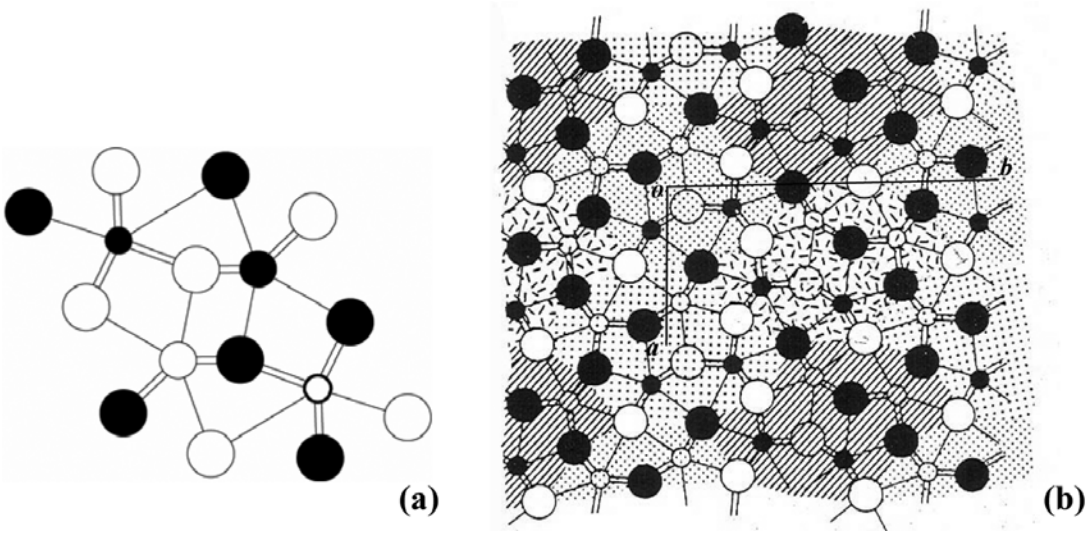

FIG. 8. a) Lozenge-like rod in galenobismutite. b) The crystal structure of Gd_2S_3 (Prewitt & Sleight 1968) interpreted as a stacking of composite rods comprising two horizontal and two vertical prisms each (CN7 and CN8). Figure in b) is from Makovicky (1992), modified.

ACKNOWLEDGEMENTS

The authors express their thanks to Carlo Garbarino for providing results of an electron-microprobe investigation and to the reviewers, Y. Moëlo and H. Effenberger, whose comments and suggestions have notably improved the manuscript. We are indebted also to Associate Editor Nigel J. Cook and to Robert F. Martin for their helpful comments. This study is part of a Ph.D. study by D.P. financed by F.S.E. – P.O.N. 2000–2006 "Ricerca Scientifica, Sviluppo Tecnologico ed Alta Formazione" Misura III.4 – Formazione superiore e Universitaria. This research was financially supported by MIUR (Ministero dell'Istruzione, dell'Università e Ricerca, Italy), CoFin 2003, project "Mineralogical and crystal-chemical investigations on lead, bismuth and arsenic sulfosalts, and secondary metal minerals" and by the Danish Research Council of Natural Science, Project Number 21.03.05.19.

REFERENCES

ARMBRUSTER, T. & HUMMEL, W. (1987): (Sb,Bi,Pb) ordering in sulfosalts: crystal-structure refinement of a Bi-rich izoklakeite. *Am. Mineral.* **72**, 821-831.

ARRIORTUA, M.I., RIUS, J., SOLÁNS, X. & AMIGÒ J.M. (1983): Thermal behavior in a synthetic phase of lead (II) – indium (III) sulphosalt: high- and low-temperature phases closely related to natural and synthetic bismuth–lead sulphosalts. *Neues Jahrb. Mineral., Monatsh.,* 343-350.

ATABAEVA, E.YA., MASHKOV, S.A. & POPOVA, S.V. (1973): Crystal structure of a new modification, Bi_2Se_3. II. *Kristallogr.* **18**, 173-174 (in Russ.).

BALIĆ-ŽUNIĆ, T. & MAKOVICKY, E. (1996): Determination of the centroid or "the best centre" of a coordination polyhedron. *Acta Crystallogr.* **B52**, 78-81.

BALIĆ-ŽUNIĆ, T. & VICKOVIĆ, I. (1996): IVTON – a program for the calculation of geometrical aspects of crystal structures and some crystal chemical applications. *J. Appl. Crystallogr.* **29**, 305- 306.

BERLEPSCH, P., ARMBRUSTER, T., MAKOVICKY, E., HEJNY, C., TOPA, D. & GRAESER, S. (2001b): The crystal structure of (001) twinned xilingolite, $Pb_3Bi_2S_6$, from Mittal–Hohtenn, Valais, Switzerland. *Can. Mineral.* **39**, 1653-1663.

BERLEPSCH, P., MAKOVICKY, E. & BALIĆ-ŽUNIĆ, T. (2001a): The crystal chemistry of meneghinite homologues and related compounds. *Neues Jahrb. Mineral., Monatsh.,* 115-135.

BERTAUT, E.F. & BLUM, P. (1956): Détermination de la structure de Ti_2CaO_4 par la méthode self-consistante d'approche directe. *Acta Crystallogr.* **9**, 121-126.

BORODAEV, Y.S., GARAVELLI, A., GARBARINO, C., GRILLO, S.M., MOZGOVA, N.N., ORGANOVA, N.I., TRUBKIN, N.V. & VURRO, F. (2000): Rare sulfosalts from Vulcano, Aeolian Islands, Italy. III. Wittite and cannizzarite. *Can. Mineral.* **38**, 23-34.

BORODAEV, Y.S., GARAVELLI, A., GARBARINO, C., GRILLO, S.M., MOZGOVA, N.N., USPENSKAYA, T.Y. & VURRO, F. (2001): Rare sulfosalts from Vulcano, Aeolian Islands, Italy. IV. Lillianite. *Can. Mineral.* **39**, 1383-1396.

BORODAEV, Y.S., GARAVELLI, A., KUZMINA, O.V., MOZGOVA, N.N., ORGANOVA, N.I., TRUBKIN, N.V. & VURRO, F. (1998): Rare sulfosalts from Vulcano, Aeolian Islands, Italy. I. Se-bearing kirkiite, $Pb_{10}(Bi,As)_6(S,Se)_{19}$. *Can. Mineral.* **36**, 1105-1114.

BORODAEV, Y.S., GARAVELLI, A., GARBARINO, C., GRILLO, S.M., MOZGOVA, N.N., PAAR, W.H., TOPA, D. & VURRO, F. (2003): Rare sulfosalts from Vulcano, Aeolian Islands, Italy. V. Selenian heyrovskýite. *Can. Mineral.* **41**, 429-440.

BRESE, N.E. & O'KEEFFE, M. (1991): Bond-valence parameters for solids. *Acta Crystallogr.* **B47**, 192-197.

BROWN, I.D. & ALTERMATT, D. (1985): Bond-valence parameters obtained from a systematic analysis of the inorganic crystal structure database. *Acta Crystallogr.* **B41**, 244-247.

BRUKER AXS (1997a): SAINT Plus, Version 6.02/NT. Bruker Analytical X-ray Systems, Inc., Madison, Wisconsin 53719, USA.

BRUKER AXS (1997b): SHELXTL, Version 5.1. Bruker Analytical X-ray Systems, Inc., Madison, Wisconsin 53719, USA.

BRUKER AXS (1998): SMART, Version 5.1. Bruker Analytical X-ray Systems, Inc., Madison, Wisconsin 53719, USA.

DECKER B.F. & KASPER J.S. (1957): The structure of calcium ferrite. *Acta Crystallogr.* **10**, 332-337.

FERRARIS, G., MAKOVICKY, E. & MERLINO, S. (2004): *Crystallography of Modular Materials*. Oxford University Press, Oxford, U.K.

GARAVELLI, A., LAVIANO, R. & VURRO, F. (1997): Sublimate deposition from hydrothermal fluids at the Fossa crater (Vulcano, Italy). *Eur. J. Mineral.* **9**, 423-432.

GARAVELLI, A., MOZGOVA, N.N., ORLANDI, P., BONACCORSI, E., PINTO, D., MOËLO, Y. & BORODAEV, Y. (2005): Rare sulfosalts from Vulcano, Aeolian Islands, Italy. VI. Vurroite, $Pb_{20}Sn_2(Bi,As)_{22}S_{54}Cl_6$, a new mineral species. *Can. Mineral.* **43**, 703-711.

HUMMEL,W. & ARMBRUSTER, T. (1987): Tl^+, Pb^{2+}, and Bi^{3+} bonding and ordering in sulfides and sulfosalts. *Schweiz. Mineral. Petrogr. Mitt.* **67**, 213-218.

IITAKA, Y. & NOWACKI, W. (1962): A redetermination of the crystal structure of galenobismutite, $PbBi_2S_4$. *Acta Crystallogr.* **15**, 691-698.

KUPČIK, V. & VESELÁ-NOVÁKOVÁ, L. (1970): Zur Kristallstruktur des Bismuthinits, Bi_2S_3. *Tschermaks Mineral. Petrogr. Mitt.* **14**, 55-59.

LIU, HUIFANG & CHANG, L.L.Y. (1994): Lead and bismuth chalcogenide systems. *Am. Mineral.* **79**, 1159-1166.

MAKOVICKY, E. (1977): Chemistry and crystallography of the lillianite homologous series. III. Crystal chemistry of lillianite homologues. Related phases. *Neues Jahrb. Mineral., Abh.* **131**, 187-207.

MAKOVICKY, E. (1981): The building principles and classification of bismuth–lead sulfosalts and related compounds. *Fortschr. Mineral.* **59**, 137-190.

MAKOVICKY, E. (1992): Crystal structures of complex lanthanide sulfides with built-in non-commensurability. *Aust. J. Chem.* **45**, 1451-1472.

MAKOVICKY, E. (1997): Modular crystal chemistry of sulfosalts and other complex sulphides. *In* Modular Aspects of Minerals (S. Merlino, ed.). *Eur. Mineral. Union, Notes in Mineral.* **1**, 237-271.

MAKOVICKY, E. & BALIĆ-ŽUNIĆ, T. (1998): New measure of distortion for coordination polyhedra. *Acta Crystallogr.* **B54**, 766-773.

MAKOVICKY, E., BALIĆ-ŽUNIĆ, T. & TOPA, D. (2001): The crystal structure of neyite, $Ag_2Cu_6Pb_{25}Bi_{26}S_{68}$. *Can. Mineral.* **39**, 1365-1376.

MAKOVICKY, E. & KARUP-MØLLER, S. (1977a): Chemistry and crystallography of the lillianite homologous series. I. General properties and definitions. *Neues Jahrb. Mineral., Abh.* **130**, 264-287.

MAKOVICKY, E. & KARUP-MØLLER, S. (1977b): Chemistry and crystallography of the lillianite homologous series. II. Definition of new minerals: eskimoite, vikingite, ourayite and treasurite. Redefinition of schirmerite and new data on the lillianite–gustavite solid-solution series. *Neues Jahrb. Mineral., Abh.* **131**, 56-82.

MUMME, W.G. (1980): Weibullite $Ag_{0.32}Pb_{5.09}Bi_{8.55}Se_{6.08}S_{11.92}$ from Falun, Sweden: a higher homologue of galenobismutite. *Can. Mineral.* **18**, 1-12.

OHSUMI, K., TSUTSUI, K., TAKEUCHI, Y. & TOKONAMI, M. (1984): Reinvestigation of the lillianite structure. *Nat. Lab. High. Energy Phys.* (*Tsukuba, Japan*), *Photon Factory Activity Rep.* **1983/1984**, VI-23.

OTTO, H.H. & STRUNZ, H. (1968): Zur Kristallchemie synthetischer Blei-Wismut-Spiessglanze. *Neues Jahrb. Mineral., Abh.* **108**, 1-19.

PREWITT, C.T. & SLEIGHT, A.W. (1968): Structure of gadolinium sesquisulfide. *Inorg. Chem.* **7**, 1090-1093.

SALANCI, B. & MOH, G. (1969): Die experimentelle Untersuchung des pseudobinären Schnitts $PbS–Bi_2S_3$ innerhalb des Pb–Bi–S–Systems in Beziehung zu natürlichen Blei-Wismut-Sulfosalzen. *Neues Jahrb. Mineral., Abh.* **112**, 63-95.

SHELDRICK, G.M. (1997): *SHELXL–97. A Program for Crystal Structure Refinement*. University of Göttingen, Göttingen, Germany.

TAKAGI, J. & TAKÉUCHI, Y. (1972): The crystal structure of lillianite. *Acta Crystallogr.* **B28**, 649-651.

TAKÉUCHI, Y. (1997): *Tropochemical Cell-Twinning: a Structure-Building Mechanism in Cristalline Solids*. Terra Scientific Publ. Co., Tokyo, Japan.

VOUTSAS, G.P. & RENTZEPERIS, P.J. (1980): The crystal structure of the paraelectric bismuth thiochloride BiSCl. *Z. Kristallogr.* **152**, 109-118.

VURRO, F., GARAVELLI, A., GARBARINO, C., MOËLO, Y. & BORODAEV, Y.S. (1999): Rare sulfosalts from Vulcano, Aeolian Islands, Italy. II. Mozgovaite $PbBi_4(S,Se)_7$, a new mineral species. *Can. Mineral.* **37**, 1499-1506.

WICKMAN, F.E. (1951): The crystal structure of galenobismutite, $PbBi_2S_4$. *Arkiv Mineral.* **1**(9), 219.

Received February 17, 2005, revised manuscript accepted Janury 1, 2006.